

Dithiolate Complexes of Manganese and Rhenium: X-ray Structure and Properties of an Unusual Mixed Valence Cluster

 $\text{Mn}_3(\text{CO})_6(\mu\text{-}\eta^2\text{-SCH}_2\text{CH}_2\text{CH}_2\text{S})_3$ Noorjahan Begum,[†] Md. Iqbal Hyder,[†] Shariff E. Kabir,^{*†} G. M. Golzar Hossain,[‡] Ebbe Nordlander,^{*§} Dalia Rokhsana,^{||} and Edward Rosenberg^{*||}

Department of Chemistry, Jahangirnagar University, Savar, Dhaka-1342, Bangladesh,
 School of Chemistry, Cardiff University, Main Building, Cardiff CF10 3AT, U.K.,
 Inorganic Chemistry, Center for Chemistry and Chemical Engineering, Lund University, Box 124,
 SE-221 00 Lund, Sweden, and Department of Chemistry, The University of Montana,
 Missoula, Montana 59812

Received June 16, 2005

Treatment of $\text{Mn}_2(\text{CO})_{10}$ with 3,4-toluenedithiol and 1,2-ethanedithiol in the presence of $\text{Me}_3\text{NO}\cdot 2\text{H}_2\text{O}$ in CH_2Cl_2 at room temperature afforded the dinuclear complexes $\text{Mn}_2(\text{CO})_6(\mu\text{-}\eta^4\text{-SC}_6\text{H}_3(\text{CH}_3)\text{S}\text{-SC}_6\text{H}_3(\text{CH}_3)\text{S})$ (**1**), and $\text{Mn}_2(\text{CO})_6(\mu\text{-}\eta^4\text{-SCH}_2\text{CH}_2\text{S}\text{-SCH}_2\text{CH}_2\text{S})$ (**2**), respectively. Similar reactions of $\text{Re}_2(\text{CO})_{10}$ with 3,4-toluenedithiol, 1,2-benzenedithiol, and 1,2-ethanedithiol yielded the dirhenium complexes $\text{Re}_2(\text{CO})_6(\mu\text{-}\eta^4\text{-SC}_6\text{H}_3(\text{CH}_3)\text{S}\text{-SC}_6\text{H}_3(\text{CH}_3)\text{S})$ (**3**), $\text{Re}_2(\text{CO})_6(\mu\text{-}\eta^4\text{-SC}_6\text{H}_4\text{S}\text{-SC}_6\text{H}_4\text{S})$ (**4**), and $\text{Re}_2(\text{CO})_6(\text{SCH}_2\text{CH}_2\text{S}\text{-SCH}_2\text{CH}_2\text{S})$ (**5**), respectively. In contrast, treatment of $\text{Mn}_2(\text{CO})_{10}$ with 1,3-propanedithiol afforded the trimanganese compound $\text{Mn}_3(\text{CO})_6(\mu\text{-}\eta^2\text{-SCH}_2\text{CH}_2\text{-CH}_2\text{S})_3$ (**6**), whereas $\text{Re}_2(\text{CO})_{10}$ gave only intractable materials. The molecular structures of **1**, **3**, and **6** have been determined by single-crystal X-ray diffraction studies. The dimanganese and dirhenium carbonyl compounds **1–5** contain a binucleating disulfide ligand, formed by interligand disulfide bond formation between two dithiolate ligands identical in structure to that of the previously reported dimanganese complex $\text{Mn}_2(\text{CO})_6(\mu\text{-}\eta^4\text{-SC}_6\text{H}_4\text{S}\text{-SC}_6\text{H}_4\text{S})$. Complex **6**, on the other hand, forms a unique example of a mixed-valence trimanganese carbonyl compound containing three bridging 1,3-propanedithiolate ligands. The solution properties of **6** have been investigated by UV–vis and EPR spectroscopies as well as electrochemical techniques.

Introduction

In recent years there has been widespread interest in transition-metal complexes containing sulfur-rich thiolate ligands not only because of their relevance to biological processes but also because of their interesting structural and catalytic properties.^{1,2} Due to the biochemical relevance, most of the early work was done on iron–thiolate compounds followed by the rapid development of the dithiolate coordination chemistry of other transition metals.^{3,4}

The use of alkane dithiolates to stabilize transition metal carbonyl cluster compounds by serving as chelating or bridging ligands, thus preventing cluster fragmentation during

reactions, has also received increasing attention. The dithiolate-bridged diiron compounds $\text{Fe}_2(\text{CO})_6(\mu\text{-S}(\text{CH}_2)_n\text{S})$ ($n = 1\text{--}4$), $\text{Fe}_2(\text{CO})_6(\mu\text{-SC}_6\text{H}_3(\text{CH}_3)\text{S})$, and $\text{Fe}_2(\text{CO})_6(\mu\text{-SC}_6\text{H}_4\text{S})$ have been reported by several groups from the reactions of

- (1) (a) *Transition Metal Sulfur Chemistry-Biological and Industrial Significance*; Stiefel, E. I., Matsumoto, K., Eds.; ACS Symposium Series 653; American Chemical Society: Washington, DC, 1996. (b) Shin, R. Y. C.; Tan, G. K.; Koh, L. L.; Goh, L. Y.; Webster, R. D. *Organometallics* **2004**, *23*, 6108. (c) Lawrence, J. D.; Rauchfuss, T. B.; Wilson, S. R. *Inorg. Chem.* **2002**, *41*, 6193. (d) Aucott, S. M.; Milton, H. L.; Robertson, S. D.; Slawin, A. M. Z.; Woollins, J. D. *Dalton Trans.* **2004**, 3347. (e) Kanney, J. A.; Noll, B. C.; DuBois, M. R. *J. Am. Chem. Soc.* **2002**, *124*, 9878. (f) Huynh, H. V.; Luggner, T.; Hahn, F. E. *Eur. J. Inorg. Chem.* **2002**, 3007. (g) Merkel, M.; Pascaly, M.; Wieting, M.; Duda, M.; Rompel, A. *Z. Anorg. Allg. Chem.* **2003**, *629*, 2216. (h) Shin, R. Y. C.; Vittal, J. J.; Zhou, Z.-Y.; Koh, L. L.; Goh, L. Y. *Inorg. Chim. Acta* **2003**, *352*, 220; (i) Shin, R. Y. C.; Vittal, J. J.; Zhou, Z.-Y.; Koh, L. L.; Goh, L. Y. *Inorg. Chim. Acta* **2004**, *357*, 635. (j) Liaw, W.-F.; Chiang, C.-Y.; Lee, G. H.; Peng, S.-M.; Lai, C.-H.; Darensbourg, M. Y. *Inorg. Chem.* **2000**, *39*, 480. (k) Shin, R. Y. C.; Bennett, M. A.; Goh, L. Y.; Chen, W.; Hockless, D. C. R.; Leong, M. K.; Mashima, K.; Willis, A. C. *Inorg. Chem.* **2003**, *42*, 46.

* Author to whom correspondence should be addressed. E-mail: ed.rosenberg@umontana.edu.

[†] Jahangirnagar University.

[‡] Cardiff University.

[§] Lund University.

^{||} The University of Montana.

$\text{Fe}_3(\text{CO})_{12}$ with the corresponding dithiols.⁴ⁱ The osmium compound $\text{Os}_2(\text{CO})_6(\mu\text{-SCH}_2\text{CH}_2\text{S})$ was obtained from the ring-opening reaction of $\text{Os}_3(\text{CO})_{12}$ with 1,4-dithiacyclohexane.^{5,6} Adams and co-workers reported the dithiolate-bridged di- and triruthenium compounds *anti*- $\text{Ru}_3(\text{CO})_7(\mu\text{-SCH}_2\text{CH}_2\text{S})_2$, *syn*- $\text{Ru}_3(\text{CO})_7(\mu\text{-SCH}_2\text{CH}_2\text{S})_2$, and $\text{Ru}_2(\text{CO})_6(\mu\text{-SCH}_2\text{CH}_2\text{S})$ from the ring-opening reaction of $\text{Ru}_3(\text{CO})_{12}$ with 1,2,5,6-tetrathiacyclooctane.⁷ We have been interested in the chemistry of group 8 transition metal carbonyl compounds containing alkanedithiolate ligands, and we have demonstrated that the reactivity of alkanedithiols toward trimetallic carbonyl clusters depends on the methylene chain length of the dithiols.^{7,8} For example, 1,2-ethanedithiol reacts with $\text{Ru}_3(\text{CO})_{12}$ at 68 °C to give $\text{Ru}_2(\text{CO})_6(\mu\text{-SCH}_2\text{CH}_2\text{S})$, whereas 1,3-propanedithiol gives $(\mu\text{-H})\text{Ru}_3(\text{CO})_{10}(\mu\text{-SCH}_2\text{CH}_2\text{CH}_2\text{S})$ and $\text{Ru}_2(\text{CO})_6(\mu\text{-SCH}_2\text{CH}_2\text{CH}_2\text{S})$. Similarly, 1,2-ethanedithiol reacts with $\text{Os}_3(\text{CO})_{10}(\text{MeCN})_2$ to give $(\mu\text{-H})\text{Os}_3(\text{CO})_{10}(\mu\text{-SCH}_2\text{CH}_2\text{SH})$, whereas 1,3-propanedithiol gives $\{(\mu\text{-H})\text{Os}_3(\text{CO})_{10}\}_2(\mu\text{-SCH}_2\text{CH}_2\text{CH}_2\text{S})$.^{8b}

A particularly interesting series of papers by Liaw et al. have appeared dealing with the reactions of $\text{Mn}_2(\text{CO})_{10}$ and $\text{Mn}(\text{CO})_5^-$ with aryl dithiolate ligands.⁹ Coordinately unsaturated mononuclear and interesting dinuclear η^4 -bis(dithiolate) complexes with S–S bonds were reported.^{9b,d} In

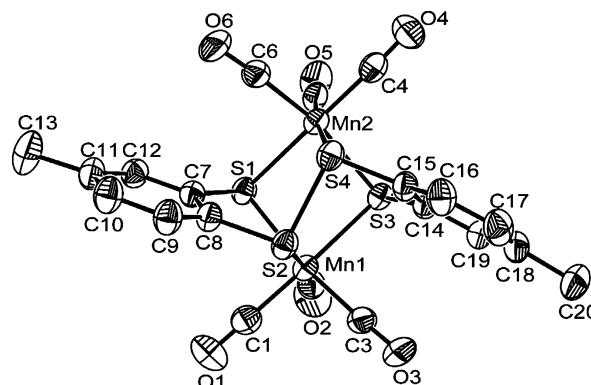


Figure 1. Molecular structure of $\text{Mn}_2(\text{CO})_6(\mu\text{-}\eta^4\text{-SC}_6\text{H}_3(\text{CH}_3)\text{S-SC}_6\text{H}_3(\text{CH}_3)\text{S})$ (**1**) showing the atom-labeling scheme; thermal ellipsoids are drawn at the 50% probability level.

addition, Adams et al. reported $\text{Mn}_2(\text{CO})_7(\mu\text{-SCH}_2\text{CH}_2\text{S})$ by the reaction of $\text{Mn}_2(\text{CO})_9(\text{MeCN})$ with 1,2-ethanedithiol.¹⁰

As a follow up to this work, we describe here the synthesis of a series of dithiolate complexes of both manganese and rhenium from the reactions of $\text{M}_2(\text{CO})_{10}$ ($\text{M} = \text{Mn, Re}$) with 3,4-toluenedithiol, 1,2-benzenedithiol ($\text{M} = \text{Re}$ only), 1,2-ethanedithiol, and 1,3-propanedithiol. The reactions of the 3,4-toluenedithiol ligand with manganese or rhenium decacarbonyl result in the formation of isomeric structures that are analogous to the previously reported manganese 1,2-benzenedithiol complex.^{9b} We have also observed a remarkable influence of the methylene chain length of the dithiol on the structure of the products formed. In the case of $\text{Mn}_2(\text{CO})_{10}$ reacting with 1,3-propanedithiol, this leads to the formation of a unique redox-active, mixed-valence cluster, which is the most significant finding of this investigation.

Results and Discussion

The reactions of $\text{Mn}_2(\text{CO})_{10}$ with 3,4-toluenedithiol and 1,2-ethanedithiol in the presence of $\text{Me}_3\text{NO}\cdot 2\text{H}_2\text{O}$ in $\text{CH}_2\text{-Cl}_2$ at room temperature afforded the dinuclear complexes $\text{Mn}_2(\text{CO})_6(\mu\text{-}\eta^4\text{-SC}_6\text{H}_3(\text{CH}_3)\text{S-SC}_6\text{H}_3(\text{CH}_3)\text{S})$ (**1**) and $\text{Mn}_2(\text{CO})_6(\mu\text{-}\eta^4\text{-SCH}_2\text{CH}_2\text{S-SCH}_2\text{CH}_2\text{S})$ (**2**) in 20 and 26% yields, respectively. **1** and **2** have been characterized by elemental analysis, IR, ^1H NMR, and mass spectroscopic data together with a single-crystal X-ray diffraction analysis for **1**.

The molecular structure of **1** is shown in Figure 1, crystal data are given in Table 1, and selected bond distances and angles are collected in Table 2. **1** contains two manganese atoms with no metal–metal bonds; the $\text{Mn}(1)\cdots\text{Mn}(2)$ distance is very long, 3.434 Å, and is clearly a nonbonding distance. Each metal center is coordinated to three S donor atoms and three terminal carbonyl groups in a distorted octahedral geometry. The most interesting aspect of this structure is the coupling of two toluenedithiolate moieties

- (2) (a) Kubo, K.; Nakano, M.; Hamaguchi, S.; Matsubayashi, G. *Inorg. Chim. Acta* **2003**, *346*, 43. (b) Cassoux, P.; Valedo, L.; Kobayashi, K.; Clark, R. A.; Underhill, A. E. *Coord. Chem. Rev.* **1991**, *110*, 115. (c) Pullen, A. E.; Oik, R.-M. *Coord. Chem. Rev.* **1999**, *188*, 211. (d) Matsubayashi, G.; Nakano, M.; Tamura, H. *Coord. Chem. Rev.* **2002**, *226*, 143. (e) Tanaka, H.; Okano, Y.; Kobayashi, H.; Suzuki, W.; Kobayashi, A. *Science* **2001**, *291*, 285. (f) Matsubayashi, G.; Ryowa, T.; Tamura, H.; Nakano, M.; Arakawa, R. *J. Organomet. Chem.* **2002**, *645*, 94.
- (3) (a) Beinert, H.; Thompson, A. J. *Arch. Biochem. Biophys.* **1983**, *222*, 333. (b) Lovenberg, W., Ed. *Iron-Sulfur Proteins*; Academic Press: New York, 1973, 1977; Vols. I–III. (c) Spiro, T. G., Ed. *Iron-Sulfur Proteins*; Wiley: New York, 1982. (d) Strasdeit, H.; Krebs, B.; Henkel, G. *Inorg. Chem.* **1984**, *23*, 1816. (e) Snyder, B. S.; Holm, R. H. *Inorg. Chem.* **1988**, *27*, 2339. (f) Huhmann-Vincent, J.; Scott, B. L.; Kubas, G. J. *Inorg. Chim. Acta* **1999**, *294*, 240. (g) Greiwe, K.; Krebs, B.; Henkel, G. *Inorg. Chem.* **1989**, *28*, 3713. (h) Dance, I. G. *Polyhedron* **1986**, *5*, 1037.
- (4) (a) Kang, B.; Hong, M.; Wen, T.; Liu, H.; Lu, J. *J. Cluster Sci.* **1995**, *6*, 379. (b) Sellman, D.; Wille, M.; Knoch, F. *Inorg. Chem.* **1993**, *32*, 2534. (c) Jiang, F.; Huang, Z.; Wu, D.; Kang, B.; Hong, M.; Liu, H. *Inorg. Chem.* **1993**, *32*, 4971. (d) Jiang, F.; Xie, X.; Hong, M.; Kang, B.; Cao, R.; Liu, H. *J. Chem. Soc., Dalton Trans.* **1993**, 1447. (e) Elduque, A.; Oro, L. A.; Pinillos, M. T.; Tiripicchio, A.; Ugozzoli, F. *J. Chem. Soc., Dalton Trans.* **1994**, 385. (f) Boorman, P. M.; Freeman, G. K. W.; Par Vez, M. *Polyhedron* **1992**, *11*, 765. (g) Henkel, G.; Krebs, B.; Betz, P.; Fietz, H.; Saatkamp, K. *Angew. Chem., Int. Ed. Engl.* **1988**, *27*, 1326. (h) Hsieh, T. C.; Nicholson, T.; Zubietta, J. *Inorg. Chem.* **1988**, *27*, 241. (i) Song, L. C. *Acc. Chem. Res.* **2005**, *38*, 21 and references therein.
- (5) (a) King, R. B. *J. Am. Chem. Soc.* **1963**, *85*, 1584. (b) Winter, A.; Zsolnai, L.; Huttner, G. *Z. Naturforsch., B: Chem. Sci.* **1982**, *37*, 1430. (c) Seyferth, D.; Womach, G. B.; Gallagher, M. K.; Cowie, M.; Hames, B. W.; Fackler, J. P., Jr.; Mazany, A. M. *Organometallics* **1987**, *6*, 283.
- (6) (a) Hasan, M. M.; Hursthouse, M. B.; Kabir, S. E.; Malik, K. M. A. *Polyhedron* **2001**, *20*, 97. (b) Kabir, S. E.; Rahman, A. F. M. M.; Parvin, J.; Malik, K. M. A. *Indian J. Chem.* **2001**, *20*, 97.
- (7) Adams, R. D.; Yamamoto, J. H. *J. Cluster Sci.* **1996**, *7*, 643.
- (8) (a) Kabir, S. E.; Johns, C. A.; Malik, K. M. A.; Mottalib, Md. A.; Rosenberg, E. *J. Organomet. Chem.* **1997**, *544*, 23. (b) Hanif, K. M.; Hursthouse, M. B.; Kabir, S. E.; Malik, K. M. A.; Mottalib, Md. A.; Rosenberg, E. *Polyhedron* **2000**, *19*, 1073. (c) Hossain, G. M. G.; Hyder, Md. I.; Kabir, S. E.; Malik, K. M. A.; Miah, Md. A.; Siddiquee, T. A. *Polyhedron* **2003**, *22*, 633. (d) Kabir, S. E.; Malik, K. M. A.; Rosenberg, E.; Siddiquee, T. A. *Inorg. Chem. Commun.* **2000**, *3*, 140.

- (9) (a) Liaw, W. F.; Hsieh, C. H.; Peng, S. M.; Lee, G. H. *Inorg. Chim. Acta* **2002**, *332*, 153. (b) Liaw, W. F.; Hsieh, C. H.; Lin, G. Y.; Lee, G. H. *Inorg. Chem.* **2001**, *40*, 3468. (c) Liaw, W. F.; Hsieh, C. H.; Lin, G. Y.; Lee, G. H.; Peng, S. M.; Lee, C. M.; Hu, C. H. *J. Chem. Soc., Dalton Trans.* **1999**, 2393. (d) Liaw, W. F.; Hsieh, C. H.; Lin, G. Y.; Lee, G. H. *Inorg. Chem.* **1998**, *37*, 6396.
- (10) Adams, R. D.; Kwon, O.-S.; Smith, M. D. *Isr. J. Chem.* **2001**, *41*, 197.

Table 1. Crystal Data for **1**, **3**, and **6**

	1	3	6
empirical formula	C ₂₀ H ₁₂ O ₆ Mn ₂ S ₄	C ₂₀ H ₁₂ O ₆ Re ₂ S ₄	C ₁₅ H ₁₈ O ₆ Mn ₃ S ₆
formula weight	586.42	848.94	651.47
<i>T</i> (K)	150(2)	150(2)	150(2)
wavelength	0.71073	0.71073	0.71073
crystal system	triclinic	triclinic	tetragonal
space group	<i>P</i> $\bar{1}$	<i>P</i> $\bar{1}$	<i>P</i> 4 ₃ 2 ₁ 2
unit cell dimensions			
<i>a</i> (Å)	9.6392(3)	9.894(3)	14.761(3)
<i>b</i> (Å)	11.1210(4)	11.157(3)	14.761(3)
<i>c</i> (Å)	12.2659(2)	12.166(4)	10.720(2)
α (deg)	112.537(2)	112.34(3)	90
β (deg)	102.680(2)	102.53(2)	90
γ (deg)	97.6174(14)	97.69(2)	90
<i>V</i> (Å ³)	1150.07(6)	1177.3(6)	2335.8(8)
<i>Z</i>	2	2	4
<i>D</i> _{calc} (g cm ⁻³)	1.693	2.395	1.853
absorption coefficient (cm ⁻¹)	1.496	10.662	2.163
<i>F</i> (000)	588	788	1308
crystal dimensions (mm)	0.25 × 0.20 × 0.20	0.45 × 0.40 × 0.30	0.45 × 0.25 × 0.22
θ range (deg)	1.88–27.47	1.89–25.17	2.35–25.15
limiting indices	–12 ≤ <i>h</i> ≤ 12 –14 ≤ <i>k</i> ≤ 14 –15 ≤ <i>l</i> ≤ 15	–11 ≤ <i>h</i> ≤ 11 –13 ≤ <i>k</i> ≤ 12 0 ≤ <i>l</i> ≤ 14	0 ≤ <i>h</i> ≤ 17 –17 ≤ <i>k</i> ≤ 0 –12 ≤ <i>l</i> ≤ 12
reflns collected	16777	4495	4558
independent reflns	5217 [<i>R</i> _{int} = 0.0459]	4236 [<i>R</i> _{int} = 0.0198]	2093 [<i>R</i> _{int} = 0.0583]
max and min transm	0.8068 and 0.7541	0.2243 and 0.1758	0.6714 and 0.5180
refinement method	full-matrix least-squares on <i>F</i> ²	full-matrix least-squares on <i>F</i> ²	full-matrix least-squares on <i>F</i> ²
data/restraints/params	5217/0/291	4236/0/291	2093/0/138
GOF on <i>F</i> ²	1.117	1.056	1.072
final <i>R</i> indices [<i>I</i> > 2σ(<i>I</i>)]	<i>R</i> 1 = 0.0374 <i>wR</i> 2 = 0.0956	<i>R</i> 1 = 0.0310 <i>wR</i> 2 = 0.0834	<i>R</i> 1 = 0.0301 <i>wR</i> 2 = 0.0734
<i>R</i> indices (all data)	<i>R</i> 1 = 0.0488 <i>wR</i> 2 = 0.1009	<i>R</i> 1 = 0.0363, <i>wR</i> 2 = 0.0853	<i>R</i> 1 = 0.0310 <i>wR</i> 2 = 0.0740
largest diff peak and hole (e Å ⁻³)	0.528 and –0.551	1.681 and –1.32	0.528 and –0.5958

Table 2. Bond Distances (Å) and Angles (deg) for Mn₂(CO)₆(μ-η⁴-SC₆H₃(CH₃)S–SC₆H₃(CH₃)S) (**1**)^a

Mn(1)–C(1)	1.811(3)	Mn(1)–C(2)	1.810(2)
Mn(1)–C(3)	1.810(3)	Mn(1)–S(2)	2.3185(6)
Mn(1)–S(1)	2.3539(7)	Mn(1)–S(3)	2.4211(6)
Mn(2)–C(5)	1.814(2)	Mn(2)–C(4)	1.815(3)
Mn(2)–C(6)	1.816(3)	Mn(2)–S(4)	2.3053(7)
Mn(2)–S(3)	2.3611(6)	Mn(2)–S(1)	2.4275(6)
S(2)–S(4)	2.2235(8)		
Mn(1)–S(1)–Mn(2)	91.80(2)	S(2)–Mn(1)–S(1)	83.30(2)
Mn(2)–S(3)–Mn(1)	91.79(2)	S(2)–Mn(1)–S(3)	95.96(2)
S(1)–Mn(1)–S(3)	82.33(2)	S(3)–Mn(2)–S(1)	82.05(2)
S(4)–Mn(2)–S(3)	83.40(2)	C(8)–S(2)–S(4)	96.18(7)
S(4)–Mn(2)–S(1)	97.03(2)	S(4)–S(2)–Mn(1)	102.26(2)
C(8)–S(2)–Mn(1)	102.65(8)	S(2)–S(4)–Mn(2)	101.50(3)

^a Symmetry transformations used to generate equivalent atoms.

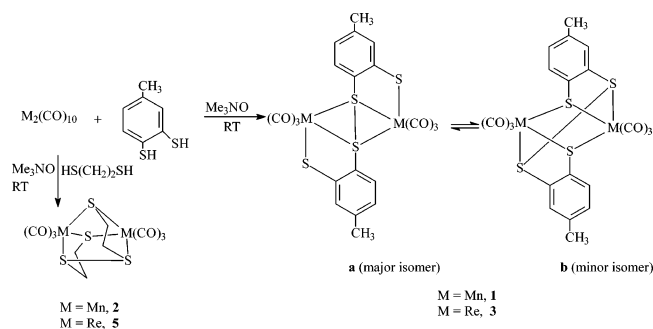
to form SC₆H₃(CH₃)S–SC₆H₃(CH₃)S. One S atom of each toluenedithiolate group bridges two Mn centers, whereas the other is coordinated to one Mn center and forms an interligand disulfide bond with the corresponding singly bonded S atom of the second toluenedithiolate moiety; the ligand in **1** is thus best described as binucleating bis-(dithiolate). In the solid-state, the disulfide ligand is found only between the sulfur atoms para to the methyl groups of the toluenedithiol ligand. The S–S bond distance, 2.2235(8) Å, of the tetrathiolate ligand is almost identical to the one previously reported for Mn₂(CO)₆(μ-η⁴-SC₆H₄S–SC₆H₄S) (2.222(1) Å)^{9b} but significantly longer than those found in Mn₂(CO)₇(μ-S₂) (2.0474(11) Å)¹¹ and Fe₂(CO)₆(μ-S₂) (2.021(3)¹² and 2.007(5) Å).¹³ The Mn–S bond distances

span a wide range, 2.3053(7)–2.4275(6) Å, but all can be regarded as Mn–S single bonds. Assuming that the disulfide ligand in **1** serves as a 10-electron donor, each metal atom achieves an 18-electron configuration without the presence of a Mn–Mn bond. The overall structure is almost identical to that found for the 1,2-benzenedithiol complex Mn₂(CO)₆(μ-η⁴-SC₆H₄S–SC₆H₄S), but the formation of the S–S bond is regioselective based on the solid-state structure.

Indeed, the ¹H NMR spectrum of **1** shows the presence of two isomers in solution in a 3:1 ratio. The aromatic region of the spectrum shows two doublets at δ 7.98 and 7.23 (d, *J* = 7.9 Hz) and a singlet at δ 7.50 for the major isomer and two doublets at δ 7.54 and 7.18 (d, *J* = 7.9 Hz) and a singlet at δ 7.94 for the minor isomer. Similarly, the aliphatic region of the spectrum contains two singlets at δ 1.50 and 1.24 for the methyl protons of the major and minor isomers, respectively. If the solid-state structure of **1** corresponds to that of the major isomer, then the minor isomer most probably has structure **1b** (Scheme 1). The two isomers differ by which thiol forms the disulfide bond. The major isomer has the S–S bond between the thiols in the para position relative to the methyl group, as in the solid state, whereas the minor isomer most likely has the disulfide bond between the thiols meta to the methyl group. In principle, there could

- (11) Adams, R. D.; Kwon, O.-S.; Smith, M. D. *Inorg. Chem.* **2002**, *41*, 6281.
 (12) Ermenko, I. L.; Berke, H.; van der Zeijden, A. A. H.; Kolobkov, B. L.; Novotorsev, V. M. *J. Organomet. Chem.* **1994**, *471*, 123.
 (13) Wei, C. H.; Dahl, L. F. *Inorg. Chem.* **1965**, *4*, 1.

Scheme 1



be a third isomer where the disulfide bond forms between one para and one meta sulfur atom, which would be expected to show two methyl signals. Apparently this isomer is formed, if at all, in concentrations too low to be detected by NMR. The two isomers could interchange by disulfide bond cleavage followed by bridge-terminal thiol exchange. This process is slow on the NMR time scale, and heating the mixture of isomers (90 °C in toluene) and then measuring NMR in CD_2Cl_2 does not change the ratio. There are two possible interpretations of this result: (1) the 3:1 ratio represents an equilibrium mixture of the two products; (2) the rate of equilibration of the two isomers is very slow on the chemical time scale. These possibilities could be differentiated by doing the variable-temperature studies in toluene and looking for a reversible change in the equilibrium constant. This possibility was precluded by the poor solubility of the complex in toluene. The difference in free energy between the two isomers is only 0.65 kcal/mol, with the structure in the solid state being slightly more stable. One can see from Figure 1 that breaking the S(2)–S(4) bond and reforming it between S(1) and S(3) would not require much reorganization of the structure. The slight preference for the para–para linkage could be due to an inductive effect of the methyl group where σ bonding with another sulfur is preferred over Mn–S bonding, where π -acceptor character is more important. This interpretation is corroborated by the ^1H NMR spectra for **2**, which shows the presence of only one isomer in solution, and by the observation of only one isomer for the previously reported 1,2-benzenedithiol analogue.^{9b} The methylene protons of the thiolate ligand in **2** are magnetically nonequivalent, appearing as four well-separated eight-line multiplets in the range δ 3.87–2.25. The well-resolved fine structure seen in the NMR spectra of these complexes is in agreement with 18-electron, diamagnetic configurations at the metal centers.

The molecular structure of **2** has been determined by a single-crystal X-ray diffraction study. However, the thin nature of the crystals resulted in data of poor quality.¹⁴ Consequently, although the gross structural features are clear, a detailed discussion of bond lengths and angles is not

(14) Crystals of **3** were monoclinic, space group $P2_1/n$, with $a = 8.777 \text{ \AA}$, $b = 13.228 \text{ \AA}$, $c = 14.341 \text{ \AA}$, $\beta = 101.33^\circ$, $\text{Mn}(1)\text{--S}(1) = 2.35 \text{ \AA}$, $\text{Mn}(2)\text{--S}(1) = 2.31 \text{ \AA}$, $\text{Mn}(1)\text{--S}(2) = 2.29 \text{ \AA}$, $\text{Mn}(1)\text{--S}(3) = 2.26 \text{ \AA}$, $\text{Mn}(1)\text{--S}(4) = 2.33 \text{ \AA}$, and $\text{Mn}(2)\text{--S}(4) = 2.34 \text{ \AA}$. They were thin needles giving weak, poor quality diffraction data (despite repeated recrystallization and data collection), and the structure could not be satisfactorily refined giving a high R1 value.

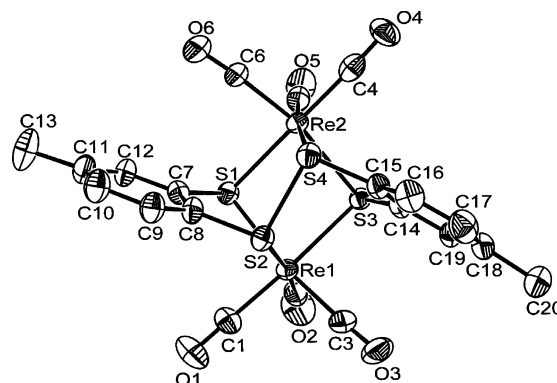


Figure 2. Molecular structure of $\text{Re}_2(\text{CO})_6(\mu\text{-}\eta^4\text{-SC}_6\text{H}_3(\text{CH}_3)\text{S-SC}_6\text{H}_3(\text{CH}_3)\text{S})$ (**3**) showing the atom-labeling scheme; thermal ellipsoids are drawn at the 50% probability level.

Table 3. Bond Distances (Å) and Angles (deg) for **3**^a

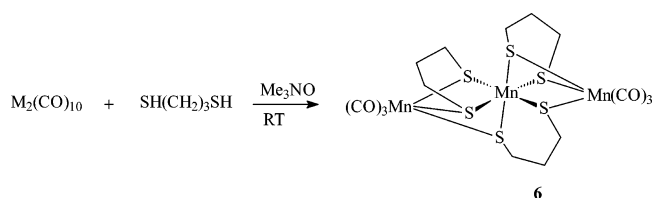
Re(1)–C(3)	1.932(7)	Re(1)–C(2)	1.923(8)
Re(1)–C(1)	1.906(7)	Re(1)–S(2)	2.436(2)
Re(1)–S(1)	2.483(2)	Re(1)–S(3)	2.539(2)
Re(2)–C(5)	1.936(8)	Re(2)–C(4)	1.918(8)
Re(2)–C(6)	1.921(7)	Re(2)–S(4)	2.425(2)
Re(2)–S(3)	2.489(2)	Re(2)–S(1)	2.542(2)
S(2)–S(4)	2.235(2)		
Re(1)–S(1)–Re(2)	93.39(6)	S(2)–Re(1)–S(1)	80.79(6)
Re(2)–S(3)–Re(1)	93.30(6)	S(2)–Re(1)–S(3)	93.81(6)
S(1)–Re(1)–S(3)	81.16(6)	S(3)–Re(2)–S(1)	80.99(6)
S(4)–Re(2)–S(3)	80.50(6)	C(8)–S(2)–S(4)	96.7(2)
S(4)–Re(2)–S(1)	95.19(6)	S(4)–S(2)–Re(1)	103.37(8)
C(8)–S(2)–Re(1)	102.7(2)	C(15)–S(4)–S(2)	94.0(2)
S(2)–S(4)–Re(2)	102.46(8)		

^a Symmetry transformations used to generate equivalent atoms.

possible. The basic structure is similar to that of **1**. The infrared spectra of **1** and **2** in the carbonyl-stretching region are very similar and indicate that all the carbonyl groups are terminal.

The reactions of $\text{Re}_2(\text{CO})_{10}$ with 3,4-toluenedithiol, 1,2-benzenedithiol, and 1,2-ethanedithiol in the presence of $\text{Me}_3\text{NO}\cdot 2\text{H}_2\text{O}$ in CH_2Cl_2 at room temperature afforded the dirhenium compounds $\text{Re}_2(\text{CO})_6(\mu\text{-}\eta^4\text{-SC}_6\text{H}_3(\text{CH}_3)\text{S-SC}_6\text{H}_3(\text{CH}_3)\text{S})$ (**3**), $\text{Re}_2(\text{CO})_6(\mu\text{-}\eta^4\text{-SC}_6\text{H}_4\text{S-SC}_6\text{H}_4\text{S})$ (**4**), and $\text{Re}_2(\text{CO})_6(\mu\text{-}\eta^4\text{-SCH}_2\text{CH}_2\text{S-SCH}_2\text{CH}_2\text{S})$ (**5**) in 18, 21, and 22% yields, respectively. **3–5** have been characterized by spectroscopic data together with single-crystal X-ray diffraction analysis for **3**. The molecular structure of **3** is shown in Figure 2, crystal data are given in Table 1, and selected bond distances and angles are given in Table 3. The molecular geometry of **3** is remarkably similar to its manganese analogue **1**. The $\text{Re}(1)\cdots\text{Re}(2)$ distance, 3.657 Å, is even longer than in **1** and is clearly a nonbonding distance. Each rhenium atom is coordinated to three terminal carbonyl ligands and three sulfur atoms. Each toluenedithiolate ligand bridges two rhenium atoms and is also bonded to the sulfur atom of the second, forming the disulfide bridge to give the binucleating bis(dithiolate) ligand. The S–S bond distance (2.235(2) Å) of the disulfide ligand is similar to that found in **1**. The Re–S bond distances span a wide range, 2.3053(7)–2.4275(6) Å, but are typical of Re–S single bonds observed in Re thiolate complexes (2.30–2.40 Å).¹⁵ Within the dithiolate ligand, the exocyclic C–S average bond length

Scheme 2



of 1.775 Å is similar in length to that of a C–S single bond and is similar to that observed for **1**.

The infrared spectra of **3**, **4**, and **5** in the carbonyl-stretching region are very similar, indicating that they are isostructural. The ¹H NMR spectrum of **3** is remarkably similar to that of **1**, indicating the presence of two isomers in solution. The major isomer shows two doublets at δ 7.93 and 7.27 (*J* = 8.0 Hz) and two singlets at δ 7.43 and 1.50, whereas the minor isomer exhibits two doublets at δ 7.48 and 7.14 (*J* = 8.0 Hz) and two singlets at δ 7.88 and 1.24. As proposed for **1**, if the solid-state structure of **3a** corresponds to the major isomer, then the minor isomer has the structure **3b** (Scheme 1). The ¹H NMR spectrum of **4** contains four equal-intensity signals, two doublets of doublets at δ 8.10 and 7.63 (*J* = 7.2, 1.6 Hz), and two doublets of triplets at δ 7.47 and 7.35 (*J* = 7.2, 1.6 Hz). The SCH₂ groups of the thiolate ligand in **5** are seen as four eight-line “multiplets” of equal intensity in the range δ 3.90–2.48. Thus, as described for **2** and the analogue of **4**, ¹H NMR spectra of **4** and **5** indicate that they exist as one isomer in solution.^{9b}

The reaction of Mn₂(CO)₁₀ with 1,3-propanedithiol in the presence of Me₃NO·2H₂O in CH₂Cl₂ at room temperature gave the trimanganese compound Mn₃(CO)₆(μ-η⁴-SCH₂CH₂CH₂S)₃ (**6**) (Scheme 2) as green crystals in 20% yield. It is less stable than **1–5** in solution, and workup must be performed under nitrogen to avoid bleaching of the color and concomitant decomposition. **6** has been characterized by a combination of spectroscopic data and single-crystal X-ray diffraction studies. The molecular structure of **6** is shown in Figure 3, crystal data are given in Table 1, and selected bond distances and angles are given in Table 4. The molecule consists of three manganese atoms, three 1,3-propanedithiolate ligands, and six carbonyl groups. Atoms Mn(2) and Mn(2′) each have three terminal carbonyl ligands, whereas the central Mn is coordinated only by six S atoms in an appropriate octahedral geometry. All of the manganese atoms are linked through μ-1,3-propanedithiolate ligands, and there are no Mn–Mn bonds. The Mn(2′)–Mn(1)–Mn(2) bond angle of 177.56(3)° indicates that the three manganese atoms are nearly linear. Each Mn atom has a slightly distorted octahedral geometry. Charge considerations require a mixed-valence Mn(IV), 2Mn(I) description, and central Mn(1) is assigned as the Mn(IV) ion and Mn(2) and Mn(2′) as Mn(I)

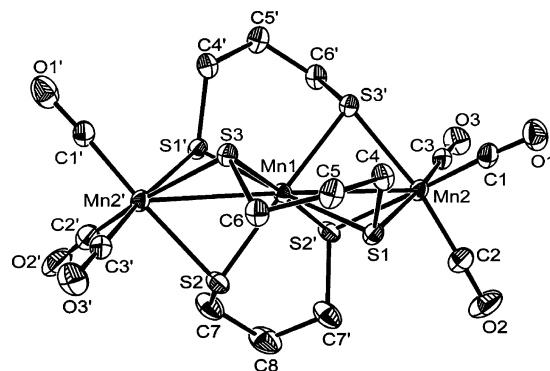


Figure 3. Molecular structure of Mn₃(CO)₆(μ-η⁴-SCH₂CH₂CH₂S)₃ (**6**) showing the atom-labeling scheme; thermal ellipsoids are drawn at the 50% probability level.

Table 4. Bond Lengths (Å) and Angles (deg) for **6**^a

Mn(1)–S(3)	2.3235(9)	Mn(1)–S(3′)	2.3235(8)
Mn(1)–S(1)	2.3400(7)	Mn(1)–S(1′)	2.3400(7)
Mn(1)–S(2)	2.3485(8)	Mn(1)–S(2′)	2.3485(8)
Mn(1)–Mn(2′)	2.9888(6)	Mn(1)–Mn(2)	2.9888(6)
Mn(2)–S(2′)	2.3865(8)	Mn(2)–S(3′)	2.3771(9)
S(2)–Mn(2′)	2.3865(8)	Mn(2)–S(1)	2.3923(9)
S(3)–Mn(2′)	2.3771(9)		
S(3)–Mn(1)–S(3′)	91.58(4)	S(3)–Mn(1)–S(1′)	86.31(3)
S(3′)–Mn(1)–S(1)	86.31(3)	S(1)–Mn(1)–S(1′)	176.57(4)
S(3′)–Mn(1)–S(1′)	96.10(3)	S(3′)–Mn(1)–S(2)	176.83(3)
S(3)–Mn(1)–S(2)	85.28(2)	S(1′)–Mn(1)–S(2)	84.19(3)
S(3)–Mn(1)–S(2′)	176.83(3)	S(3′)–Mn(1)–S(2′)	85.28(2)
S(1)–Mn(1)–S(2′)	84.19(3)	S(1′)–Mn(1)–S(2′)	93.55(3)
S(2)–Mn(1)–S(2′)	97.86(4)	S(3)–Mn(1)–Mn(2′)	51.32(2)
S(3′)–Mn(1)–Mn(2′)	126.54(3)	S(1)–Mn(1)–Mn(2′)	128.48(2)
S(1′)–Mn(1)–Mn(2′)	51.61(2)	S(2)–Mn(1)–Mn(2′)	51.43(3)
S(2′)–Mn(1)–Mn(2′)	130.65(2)	S(3)–Mn(1)–Mn(2)	126.54(3)
S(3′)–Mn(1)–Mn(2)	51.32(2)	S(1)–Mn(1)–Mn(2)	51.61(2)
S(1′)–Mn(1)–Mn(2)	128.84(2)	S(2)–Mn(1)–Mn(2)	130.65(2)
S(2′)–Mn(1)–Mn(2)	51.43(2)	Mn(2′)–Mn(1)–Mn(2)	177.56(3)
S(2′)–Mn(2)–S(1)	82.24(3)	S(3′)–Mn(1)–S(2′)	83.27(3)
S(3′)–Mn(2)–Mn(1)	49.73(2)	S(3′)–Mn(2)–S(1)	83.94(3)
S(1)–Mn(2)–Mn(1)	50.06(2)	S(2′)–Mn(2)–Mn(1)	50.30(2)
Mn(1)–S(2)–Mn(2′)	78.28(2)	Mn(1)–S(1)–Mn(2)	78.33(2)
S(3)–Mn(1)–S(1)	96.10(3)	Mn(1)–S(3)–Mn(2′)	78.95(3)

^a Symmetry transformations used to generate equivalent atoms.

ions on the basis of their structural parameters. The Mn···Mn separations (2.9888(6) Å) are much shorter than those in **1** (3.434 Å) and **3** (3.657 Å), owing to the increase in the number of bridging atoms, but the 2.9888(6) Å value is still too long for direct Mn–Mn bonding (<2.7 Å).¹⁰ The Mn(2)–S and Mn(2′)–S bond distances span a wide range, 2.3053(7)–2.4275(6) Å, but are similar to those found in other manganese sulfido carbonyl complexes.¹¹ The Mn(1)–S distances (2.3235(8)–2.3400(7) Å) are shorter compared to the Mn–S(2/2′) distances (2.3771(9)–2.3923(9) Å) but span a much narrower range. The infrared spectrum of **6** exhibits absorption bands at 2012 and 1925 cm^{−1}, indicating that the carbonyl groups are terminal. The UV–vis spectrum of **6** shows absorption maxima in the visible region at 484, 620, and 780 nm and two bands at 381 and 389 nm (Figure 4). Although the general appearance of the spectrum is similar to other d³ complexes,¹⁶ it would not be appropriate to assign these bands. A more detailed spectroscopic investigation of the observed transitions, and perhaps

(15) (a) Herberhold, M.; Jin, G. X.; Milius, W. *J. Organomet. Chem.* **1996**, 512, 111. (b) Herberhold, M.; Jin, G. X.; Milius, W. *Z. Anorg. Allg. Chem.* **1994**, 620, 1295. (c) Lente, G.; Guzei, I. A.; Espenson, J. H. *Inorg. Chem.* **2000**, 39, 1311. (d) Jacob, J.; Guzei, I. A.; Espenson, J. H. *Inorg. Chem.* **1999**, 38, 3266.

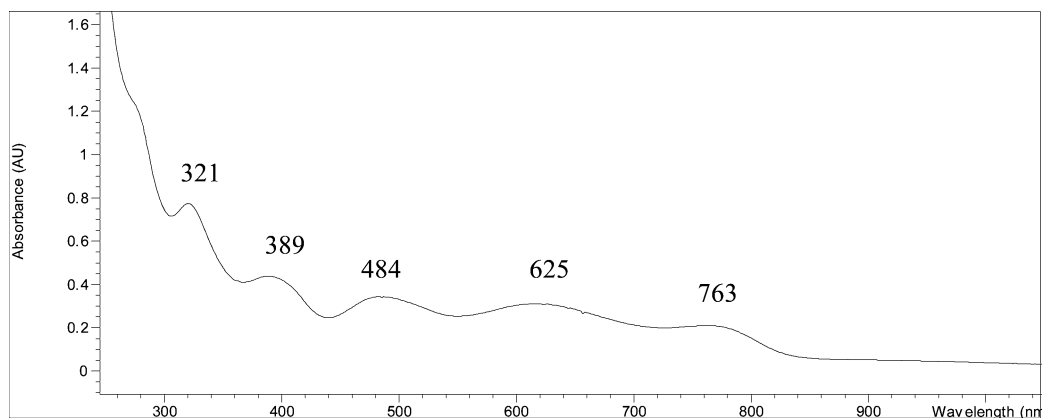


Figure 4. UV-visible absorption spectrum of $\text{Mn}_3(\text{CO})_6(\mu\text{-}\eta^4\text{-SCH}_2\text{CH}_2\text{CH}_2\text{S})_3$ (**6**) in CH_2Cl_2 .

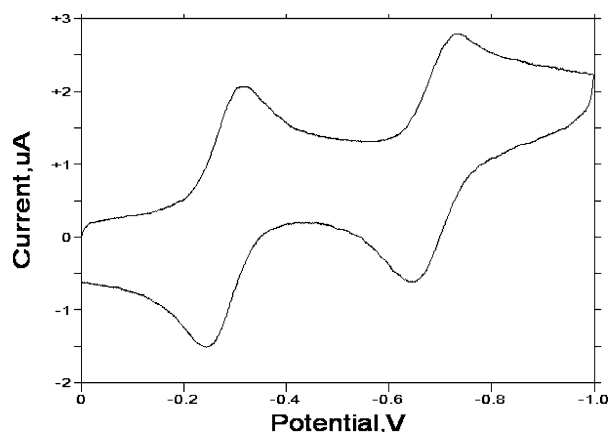


Figure 5. Cyclic voltammogram of $\text{Mn}_3(\text{CO})_6(\mu\text{-}\eta^4\text{-SCH}_2\text{CH}_2\text{CH}_2\text{S})_3$ (**6**) in CH_2Cl_2 at 50 mV/s scan rate vs Ag/AgCl.

a computational study, would be necessary in order to understand the contributions of the Mn(I) centers to the spectrum.

In an attempt to obtain the rhenium analogue of **6**, we reacted $\text{Re}_2(\text{CO})_{10}$ with 1,3-propanedithiol in the presence of $\text{Me}_3\text{NO}\cdot 2\text{H}_2\text{O}$ in CH_2Cl_2 at room temperature. Workup of the resulting yellow solution, followed by chromatographic separation, gave several very minor bands which could not be characterized completely. The reaction also gave a green solution, but the color fades within seconds after applying it to silica for chromatographic separation, suggesting a decrease in stability with increasing chain length of the dithiol.

Cyclic voltammetry of **6** shows two reversible one-electron reductions at half-wave potentials of -0.80 and -1.223 V vs Fc/Fc^+ at a scan rate of 50 mV/s (Figure 5). The values of these half-wave potentials are at much more negative values than for similar redox couples in aqueous solutions,¹⁷ but the second reduction potential is similar to that observed for the Mn(III)/Mn(II) couple in mononuclear dithiolate complexes in the same solvent.^{3g} However, the reduction potentials for the latter complexes are irreversible, whereas those for **6** are reversible even at relatively slow

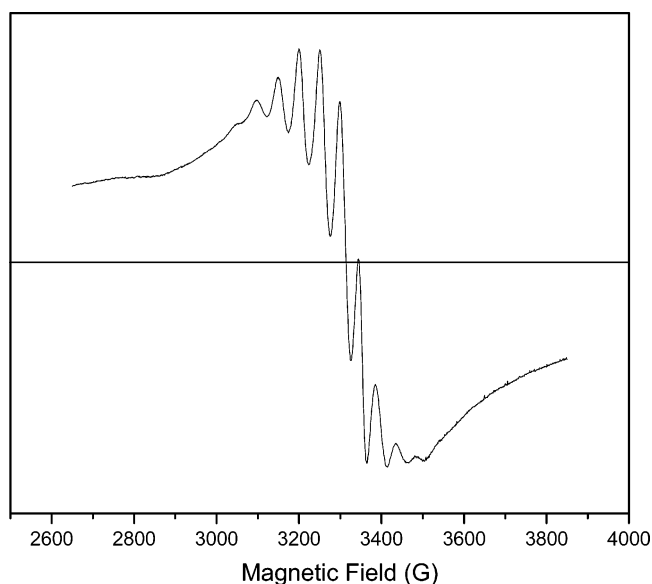


Figure 6. ESR spectrum of $\text{Mn}_3(\text{CO})_6(\mu\text{-}\eta^4\text{-SCH}_2\text{CH}_2\text{CH}_2\text{S})_3$ (**6**) in CH_2Cl_2 ; parameters used: 3250 center field, 1200 sweep width, 9.331 GHz frequency, 3.99 e4 gain, 15 G amplitude, 10 scans at 77 K.

scan rates (50 mV/s). This suggests that the bridging sulfido ligands and the adjacent metal carbonyl centers stabilize the reduced species via delocalization and dative π bonding, respectively.

The ESR spectrum of **6** shows a partially resolved six-line signal (Figure 6) with an isotropic g value = 2, which indicates an octahedral ligand field around the Mn(IV) ion.¹⁸ The hyperfine coupling constant is ~ 50 G and is similar to that reported for the neutral mononuclear tetraazideomanganese(IV) complex $\text{Mn}(\text{bpy})(\text{N}_3)_4$ (bpy = 2,2'-bipyridine).¹⁸ Taken together, the visible spectrum and the ESR data suggest a near-perfect octahedral environment for the central manganese in **6** in solution on the electronic time scale.

Conclusions

The influence of the methylene chain length on the reactivity of dithiols toward $\text{Mn}_2(\text{CO})_{10}$ and $\text{Re}_2(\text{CO})_{10}$ has been demonstrated. The synthetic route developed for the dinuclear disulfide complexes **1–5** of Mn and Re from the reactions of $\text{Mn}_2(\text{CO})_{10}$ and $\text{Re}_2(\text{CO})_{10}$ with 3,4-toluene-

(16) Huheey, J. E.; Keiter, E. A.; Keiter, R. L. *Inorganic Chemistry*, 4th ed; Harper-Collins: New York, 1993; p 447.

(17) Brudvig, G. W.; Thorp, H. H.; Crabtree, R. H. *Acc. Chem. Res.* **1991**, *24*, 311 and references therein.

(18) Dave, B. C.; Czernuszewicz, R. S. *J. Coord. Chem.* **1994**, *33*, 257.

dithiol, 1,2-benzenedithiol, and 1,2-ethanedithiol represent direct routes to this ligand system, whereas the previously reported 1,2-benzenedithiol analogue of **1** was obtained by protonation of an intermediate $\text{Mn}(\text{CO})_3(1,2\text{-S}_2\text{C}_6\text{H}_4)$ associated with the liberation of hydrogen.^{9b} Indeed, such mononuclear intermediates may be involved in the reactions reported here, but the unsaturated species created by the amine oxide encourage rapid secondary reactions and prevent their isolation. **1** and **3**, which are 3,4-toluenedithiol derivatives, exist as two isomers in solution, brought about by the disposition of the disulfide bond relative to the methyl groups on the benzene ring, whereas **2**, **4**, and **5** exist as a single isomer. In sharp contrast, 1,3-propanedithiol reacts with $\text{Mn}_2(\text{CO})_{10}$ to give the mixed-valence (Mn(I)/Mn(IV)/Mn(I)) trimanganese carbonyl compound **6**, containing three bridging 1,3-propanedithiolate ligands. The overall geometry observed for **6** is similar to that seen for the related Mn(II)/Mn(III)/Mn(II) trimanganese propanedithiolate complex $[\text{PPN}]_2[\text{Mn}_3(\mu\text{-SCH}_2\text{CH}_2\text{CH}_2\text{S})_3]$, except that the geometry around the central Mn is highly distorted, as would be expected for a d^4 electron configuration.¹⁹ In addition, related Mn(II)/Mn(IV)/Mn(II) clusters containing the dipyriddy ketoneoxime ligand have been reported where the central Mn(IV) has an almost-perfect octahedral geometry as for **6**.²⁰ The oxidation of the Mn centers observed in the formation of all of the reported complexes is undoubtedly associated with the liberation of dihydrogen (or water with the aid of air oxidation), and the formation of the Mn(IV) center in **6** is probably driven by the suitability of the three-carbon chain for formation of an octahedral geometry by reaction of $(\text{CO})_3\text{Mn}(\text{SCH}_2\text{CH}_2\text{CH}_2\text{SH})_3$ with a dinuclear complex similar to **1**. The fact that the complex analogous to **6** is not formed in the case of rhenium and the lack of formation of dinuclear species with propanedithiol are more difficult to rationalize but may be the result of a combination of the reduction potential of the dithiol and the stronger Re–CO bonds. **6** provides a potentially useful mildly oxidizing cluster which could have applications in redox catalysis.

Experimental Section

General Procedures. Unless otherwise stated, all reactions were carried out under nitrogen atmosphere using standard Schlenk techniques. Reagent grade solvents were freshly distilled from appropriate drying agents and degassed prior to use. Infrared spectra were recorded on a Shimadzu FTIR 8101 spectrophotometer. UV–vis spectra were recorded on a Perkin-Elmer Lambda 11 spectrometer. EPR spectra were recorded on a Bruker EMX spectrometer. NMR spectra were recorded on a Bruker DPX 400 instrument. Elemental analyses were performed by Schwarzkopf Microanalytical Laboratories, Woodside, New York. $\text{Mn}_2(\text{CO})_{10}$ and $\text{Re}_2(\text{CO})_{10}$ were purchased from Strem Chemicals, and 3,4-toluenedithiol, 1,2-ethanedithiol, and 1,3-propanedithiol were from Aldrich and used as received. Fast atom bombardment mass spectra were

obtained on a JEOL SX-102 spectrometer using 3-nitrobenzyl alcohol as matrix and CsI as a calibration standard.

Reaction of $\text{Mn}_2(\text{CO})_{10}$ with 3,4-Toluenedithiol. $\text{Me}_3\text{NO}\cdot 2\text{H}_2\text{O}$ (0.114 g, 1.025 mmol) was added to a CH_2Cl_2 solution (50 mL) of $\text{Mn}_2(\text{CO})_{10}$ (0.200 g, 0.513 mmol) and stirred for 10 min. 3,4-Toluenedithiol (0.160 g, 1.024 mmol) was then added to the reaction mixture and stirred for a further 20 min at room temperature. The color of the reaction mixture changed from orange to red. The solution was filtered through a short silica column to remove excess Me_3NO . The solvent was removed under reduced pressure, and the residue was separated by TLC on silica gel. Elution with hexane/ CH_2Cl_2 (10:1, v/v) gave one major and several very minor bands. The major band afforded $\text{Mn}_2(\text{CO})_6(\mu\text{-}\eta^4\text{-SC}_6\text{H}_3(\text{CH}_3)\text{S}-\text{SC}_6\text{H}_3(\text{CH}_3)\text{S})$ (**1**) (0.061 g, 20%) as red crystals from hexane/ CH_2Cl_2 at -20°C . Anal. calcd for $\text{C}_{20}\text{H}_{12}\text{O}_6\text{Mn}_2\text{S}_4$: C, 40.96; H, 2.06. Found: C, 41.12; H, 2.22. IR (ν_{CO} , CH_2Cl_2): 2039 s, 2019 vs, 1963 m, 1942 cm^{-1} , ^1H NMR (CD_2Cl_2): major isomer, δ 7.98 (d, 1 H, $J = 8.0$ Hz), 7.50 (s, 1H), 7.23 (d, 1H, $J = 8.0$ Hz), 1.50 (s, 3H); minor isomer, δ 7.94 (s, 1H), 7.54 (d, 1 H, $J = 8.0$ Hz), 7.18 (d, 1H, $J = 7.98$ Hz), 1.24 (s, 3H). FAB MS: m/z 586.

Reaction of $\text{Mn}_2(\text{CO})_{10}$ with 1,2-Ethanedithiol. A similar reaction of $\text{Mn}_2(\text{CO})_{10}$ (0.255 g, 0.654 mmol), 1,2-ethanedithiol (0.127 g, 1.295 mmol), and $\text{Me}_3\text{NO}\cdot 2\text{H}_2\text{O}$ (0.176 g, 1.583 mmol) followed by similar workup and chromatographic separation afforded $\text{Mn}_2(\text{CO})_6(\mu\text{-}\eta^4\text{-SCH}_2\text{CH}_2\text{S}-\text{SCH}_2\text{CH}_2\text{S})$ (**2**) as orange crystals (0.080 g, 26%) from hexane/ CH_2Cl_2 at -20°C . Anal. calcd for $\text{C}_{10}\text{H}_8\text{Mn}_2\text{O}_6\text{S}_4$: C, 25.98; H, 1.74. Found: C, 26.25; H, 1.88. IR (ν_{CO} , CH_2Cl_2): 2037 s, 2016 vs, 1956 s, 1927 cm^{-1} , ^1H NMR (CD_2Cl_2): δ 3.87 (8-line m, 2H), 3.43 (8-line m, 2H), 2.48 (8-line m, 2H), 2.25 (8-line m, 2H). FAB MS: m/z 462.

Reaction of $\text{Re}_2(\text{CO})_{10}$ with 3,4-Toluenedithiol. $\text{Me}_3\text{NO}\cdot 2\text{H}_2\text{O}$ (0.136 g, 1.223 mmol) was added to a CH_2Cl_2 solution (50 mL) of $\text{Re}_2(\text{CO})_{10}$ (0.400 g, 0.61 mmol) and stirred for 10 min, after which 3,4-toluenedithiol (0.192 g, 1.228 mmol) was added to the reaction mixture and stirred for a further 30 min at room temperature. The solution was filtered through a short silica column. The solvent was removed under reduced pressure, and the residue was chromatographed by TLC on silica gel. Elution with hexane/ CH_2Cl_2 (3:1, v/v) gave one main and several minor bands. The major band afforded $\text{Re}_2(\text{CO})_6(\mu\text{-}\eta^4\text{-SC}_6\text{H}_3(\text{CH}_3)\text{S}-\text{SC}_6\text{H}_3(\text{CH}_3)\text{S})$ (**3**) (0.094 g, 18%) as red crystals from hexane/ CH_2Cl_2 at room temperature. Anal. calcd for $\text{C}_{20}\text{H}_{12}\text{O}_6\text{Re}_2\text{S}_4$: C, 28.29; H, 1.42. Found: C, 28.48; H, 1.52. IR (ν_{CO} , CH_2Cl_2): 2042 s, 2025 vs, 1954 m, 1931 cm^{-1} , ^1H NMR (CD_2Cl_2): major isomer, δ 7.93 (d, 1 H, $J = 8.0$ Hz), 7.43 (s, 1H), 7.27 (d, 1H, $J = 8.0$ Hz), 1.50 (s, 3H); minor isomer δ 7.88 (s, 1H), 7.48 (d, 1 H, $J = 8.0$ Hz), 7.14 (d, 1H, $J = 8.0$ Hz), 1.24 (s, 3H). FAB MS: m/z 850.

Reaction of $\text{Re}_2(\text{CO})_{10}$ with 1,2-Benzenedithiol. A similar reaction to that above of $\text{Re}_2(\text{CO})_{10}$, 1,2-benzenedithiol, and $\text{Me}_3\text{NO}\cdot 2\text{H}_2\text{O}$ followed by similar chromatographic separation gave $\text{Re}_2(\text{CO})_6(\mu\text{-}\eta^4\text{-SC}_6\text{H}_4\text{S}-\text{SC}_6\text{H}_4\text{S})$ (**4**) (0.106 g, 21%) as red crystals from hexane/ CH_2Cl_2 at -20°C . Anal. calcd for $\text{C}_{18}\text{H}_8\text{O}_6\text{Re}_2\text{S}_4$: C, 26.34; H, 0.98. Found: C, 26.48; H, 1.22%. IR (ν_{CO} , CH_2Cl_2): 2045 s, 2026 vs, 1958 s, 1933 cm^{-1} , ^1H NMR (CD_2Cl_2): δ 8.10 (dd, 1 H, $J = 7.6, 1.2$ Hz), 7.63 (dd, 1 H, $J = 7.6, 1.2$ Hz), 7.47 (dt, 1 H, $J = 7.6, 1.2$ Hz), 7.35 (dt, 1 H, $J = 7.6, 1.2$ Hz). FAB MS: m/z 820.

Reaction of $\text{Re}_2(\text{CO})_{10}$ with 1,2-Ethanedithiol. A similar reaction of $\text{Re}_2(\text{CO})_{10}$, 1,2-ethanedithiol, and $\text{Me}_3\text{NO}\cdot 2\text{H}_2\text{O}$ followed by a similar workup and chromatographic separation but eluting with hexane/ CH_2Cl_2 (7:3, v/v) gave one major band which afforded $\text{Re}_2(\text{CO})_6(\mu\text{-}\eta^4\text{-SCH}_2\text{CH}_2\text{S}-\text{SCH}_2\text{CH}_2\text{S})_2$ (**5**) (0.100 g, 22%) as orange crystals from hexane/ CH_2Cl_2 at room temperature.

(19) Seela, J.; Knapp, M. J.; Kolack, K. S.; Chang, H. R.; Huffman, J. C.; Hendrickson, D. N.; Christou, G. *Inorg. Chem.* **1998**, *37*, 516.

(20) (a) Alexiou, M.; Dendrinou-Samara, C.; Karagianni, A.; Biswas, S.; Zaleski, C. M.; Kampf, J.; Yoder, D.; Penner-Hahn, J. E.; Pecoraro, V. L.; Kessissoglou, D. P. *Inorg. Chem.* **2003**, *42*, 2185. (b) Alexiou, M.; Zaleski, C. M.; Dendrinou-Samara, C.; Kampf, J.; Kessissoglou, D. P. *Z. Anorg. Allg. Chem.* **2003**, *629*, 2348.

Anal. calcd for $C_{10}H_8O_6Re_2S_4$: C, 16.57; H, 1.11. Found C, 16.71; H, 1.22. IR (ν_{CO} , CH_2Cl_2): 2040 s, 2021 vs, 1948 m, 1919 m cm^{-1} , 1H NMR (CD_2Cl_2): δ 3.90 (7-line m, 2H), 3.58 (8-line m, 2H), 3.04 (7-line m, 2H), 2.48 (8-line m, 2H). FAB MS: m/z 724.

Reaction of $Mn_2(CO)_{10}$ with 1,3-Propanedithiol To a CH_2Cl_2 solution (20 mL) of $Mn_2(CO)_{10}$ (0.259 g, 0.664 mmol) and 1,3-propanedithiol (0.139 g, 1.284 mmol) was added dropwise a CH_2Cl_2 solution (30 mL) of $Me_3NO \cdot 2H_2O$ (0.216 g, 1.943 mmol) (15 mL) over a period of 15 min. The reaction mixture was stirred under nitrogen for a further 30 min. Workup of the reaction mixture as above followed by chromatographic separation on silica gel TLC plates eluting with hexane/acetone (3:2, v/v) developed one major green band and one very minor band. The major green band afforded $Mn_3(CO)_6(\mu-\eta^4-SCH_2CH_2CH_2S)_3$ (**6**) as green crystals (0.053 g, 20%) from hexane/ CH_2Cl_2 at $-20^\circ C$. Anal. Calcd. for $C_{15}H_{18}Mn_3O_6S_6$: C, 27.65; H, 2.78. Found: C, 27.78; H, 3.06. IR (ν_{CO} , CH_2Cl_2): 2012 vs, 1938 s cm^{-1} . MS: m/z 651. The minor band was too small for complete characterization.

Attempted Reaction of $Re_2(CO)_{10}$ with 1,3-Propanedithiol. $Me_3NO \cdot 2H_2O$ (0.141 g, 1.26 mmol) was added to a solution of $Re_2(CO)_{10}$ (0.400 g, 0.61 mmol) in CH_2Cl_2 (50 mL) and 1,3-propanedithiol (0.132 g, 1.22 mmol), and the reaction mixture was stirred for 1 h and 15 min at room temperature. Workup as above gave several very minor bands, each of which was too small for complete characterization.

X-ray Crystallography. Crystals of **1**, **3**, and **6**, suitable for diffraction analysis, were grown by slow evaporation from a hexane/methylene chloride solution at $-4^\circ C$. Crystallographic data were collected using a FAST area detector diffractometer and Mo $K\alpha$ radiation ($\lambda = 0.71073 \text{ \AA}$) according to previously described procedures.²¹ The unit cell parameters were determined by the least-squares refinement of the diffractometer angles for 250 reflections, and the data were corrected for absorption using DIFABS.²² The structures were solved by direct methods (SHELXS-97)²³ and refined on F^2 by full-matrix least-squares (SHELXL-97)²⁴ using

all unique data. All non-hydrogen atoms were refined anisotropically. The hydrogen atoms were included in calculated positions (riding model). The crystal data and refinement details for **1**, **3**, and **6** are summarized in Table 1.

Electrochemistry. Electrochemical measurements were performed with a BAS CV-50W analyzer equipped with a standard three-electrode cell. This cell was designed to allow the tip of the reference electrode to closely approach the working electrode. Voltammetric experiments were performed using Ag/AgCl as the reference electrode, a glossy carbon as the working electrode, and platinum wire as the auxiliary electrode. Typically, a solution containing 1 mM of the cluster and 0.1 M of the supporting electrolyte (tetrabutylammonium hexafluorophosphate, Bu_4NPF_6) was prepared using freshly distilled methylene chloride. The solutions used for electrochemical measurements were deoxygenated with an argon purge and kept under argon flux during the measurements. CH_2Cl_2 was freshly distilled from phosphorus pentoxide.

Acknowledgment. The Swedish International Development Agency (SIDA) and the Swedish Research Council (VR) are gratefully acknowledged for supporting the collaboration between S.E.K. and E.N. We are thankful to Doreen Brown at Montana State University for recording the ESR spectra. Support for this research by the Department of Energy (E.R., Grant No. DE-FG02-01ER45869) is also acknowledged.

Supporting Information Available: Tables of crystal data and data collection parameters, atomic coordinates, anisotropic displacement parameters, and bond lengths and angles for **1**, **3**, and **6**. X-ray crystallographic files in CIF format for **1**, **4**, and **7**. This material is available free of charge via the Internet at <http://pubs.acs.org>.

IC050987B

(21) Darr, A.; Drake, S. R.; Hursthouse, M. B.; Malik, K. M. A. *Inorg. Chem.* **1993**, *32*, 5704.

(22) Walker, N. P. C.; Stuart, D. *Acta Crystallogr., Sect. A: Found. Crystallogr.* **1983**, *39*, 158.

(23) Sheldrick, G. M. *Acta Crystallogr., Sect. A: Found. Crystallogr.* **1990**, *46*, 467.

(24) Sheldrick, G. M. *SHELXL-97 Program for Crystal Structure Refinement*; University of Göttingen: Germany, 1997.